

Attenuated Total Internal Reflection Infrared Mapping Microspectroscopy Using an Imaging Microscope

ANDRÉ J. SOMMER,* LOUIS G. TISINGER, CURTIS MARCOTT, and GLORIA M. STORY

Molecular Microspectroscopy Laboratory, Department of Chemistry and Biochemistry, Miami University, Oxford, Ohio 45056 (A.J.S., L.G.T.); and The Procter and Gamble Company, Miami Valley Laboratories, Cincinnati, Ohio 45239 (C.M., G.M.S.)

Attenuated total internal reflection (ATR) infrared mapping microspectroscopy using an infrared microscope and a focal plane array is investigated and reported. The study demonstrates the advantages of conducting ATR microspectroscopy using a focal plane array detector. These benefits include the rapid acquisition of molecular specific images, ease of sample preparation, and increased spatial resolution. An experimental determination of the spatial resolution found that the combined system operates very close to the diffraction limit, and a 4× magnification factor associated with the germanium internal reflection element was realized. Experiments conducted on several polymer samples and a biological sample demonstrate the future viability of the method.

Index Headings: Imaging microspectroscopy; ATR microspectroscopy; Fiber analysis; Polymer analysis; Focal plane array.

INTRODUCTION

Attenuated total internal reflection (ATR) infrared spectroscopy and microspectroscopy continue to increase in popularity due to the fact that little sample preparation is required and the method's inherent surface sensitivity (small optical pathlength) allows highly absorbing samples to be analyzed. The relatively new small-element single-bounce geometry not only enhances the signal throughput of a measurement but also affords the ability to measure micrometer-sized samples.¹ Currently, all the major manufacturers of infrared accessories offer devices based on a single-bounce geometry. More recently, a portable ATR microsampling instrument was introduced at the 2000 Pittsburgh Conference and Exposition. Although the device, which incorporates a video microscope for viewing and an integrated interferometer, was targeted for drug identification and trace analysis in field forensics, its capabilities are equally suited for the industrial analytical laboratory.² In the research environment, ATR microspectroscopy affords the analyst the ability to obtain information on spatial domains that are at or below the wavelength of light employed in the analysis.^{3–5} This capability arises from the fact that the sample is immersed in a medium of high refractive index, i.e., the

internal reflection element (IRE). Consequently, the diffraction-limited spot size at the microscope's focus is reduced, thereby increasing spatial resolution. Moreover, the collection efficiency of light is improved, which increases the throughput of the measurement. The magnification factor associated with the refractive index (n) of the internal reflection element allows one to work with aperture sizes that are n times larger, thereby eliminating diffraction effects introduced by small aperture dimensions.^{4,5}

Attempts to employ these advantages have mainly focused on mapping experiments where information on small spatial domains of a large sample is desired. One of the first groups to describe such a technique was that of Nakano and Kawata, who constructed a purpose-built evanescent-field scanning microscope.³ These researchers employed a germanium hemisphere as the IRE and proposed two configurations for its use. The first configuration involved translating the sample beneath the hemisphere to obtain the desired maps. However, this configuration requires that the sample be held in close proximity (ca. less than 1 μm) to the IRE during the scan. Due to this constraint, the authors chose the second configuration, which involved attaching the sample to the base of the hemisphere. The IRE and sample were then placed at the focus of the infrared microscope and scanned off-axis to yield infrared maps. The system was confocal in that both the source and sample images were apertured. Using this geometry, the authors were able to demonstrate submicrometer spatial resolution. One drawback to this approach is that the source or detector must be scanned in unison with the IRE/sample to produce the confocal maps. Lewis and Sommer later investigated a similar approach using a conventional infrared microscope.⁵ This system employed global illumination and a single aperture placed at the primary image plane of the microscope. The basis for using such a system was that only the IRE/sample need be translated, circumventing the movement of the source or detector at the same time. Although improved spatial resolution was observed, compared to a transmission measurement, it was necessary to record the sample spectrum at the precise off-axis location as the background spectrum. This requirement

Received 25 August 2000; accepted 14 November 2000.

* Author to whom correspondence should be sent.

was necessary to overcome aberrations associated with off-axis positions and made the measurement of an image a lengthy process.

A solution to some of the difficulties experienced by these researchers is the use of an infrared microscope in which the detector is a focal plane array. In these microscopes, as in Raman microscopes using charge-coupled detectors (CCDs), the detector element serves as the area-defining aperture.⁶ The combination of detector element size, microscope numerical aperture, and magnification from the sample to detector plays an important role in the spatial resolution that can be achieved. From the standpoint of ATR microspectroscopy, each detector element (pixel) on the focal plane array is imaged or corresponds to a position on the sample and vice versa. As a result, there is no need to move the IRE/sample pair beneath the microscope in order to obtain an infrared map or image provided that global illumination is employed. We report on what we believe is the first demonstration of ATR mapping microspectroscopy using a microscope possessing a focal plane array detector. The overall benefits of this approach are demonstrated and system parameters are verified by using samples having known geometries.

EXPERIMENTAL

The spectra were collected with a Bio-Rad-Digilab Division StingRay imaging system, which consisted of a UMA 500 microscope, an FTS-60A step-scanning Fourier transform infrared (FT-IR) spectrometer, and a 64×64 mercury cadmium telluride (MCT) focal plane array. A four-position cold filter wheel (Kadel) was mounted on the entrance aperture of the detector, and a long-pass optical filter was employed to limit the spectral range from 1800 to 900 cm^{-1} . An optical diagram of the microscope is shown in Fig. 1.

The internal reflection elements employed in this investigation are the germanium cartridges (Model # USS-ATR-J) used on a Harrick Scientific Split Pea ATR microsampling accessory. Details on their modification and use for infrared microspectroscopy have been reported earlier.⁴ Since no energy meter was available on the system and the contrast between an aligned IRE and misaligned IRE was rather small, an auxiliary method to align the crystals had to be developed. This procedure was done by employing a cartridge without the crystal and the one on which the sample would actually be collected. A mirror was placed on the cartridge without the crystal, and the assembly was placed on the microscope stage with its long axis perpendicular to the observer. With the use of visible reflectance illumination, the mirror could be viewed through the cartridge housing and aligned on all three axes. The illuminated area appeared as an oval with its long axis perpendicular to the observer. The cartridge was then carefully replaced by the IRE with the sample clamped to its base. During early experiments, it was noted that, although the X and Y positions were correct, the Z position was not optimal. The optimal Z position was determined by using a conventional infrared microscope in the energy mode and noting the difference in Z positions for the cartridge with the mirror mounted and that with the IRE. This difference was then

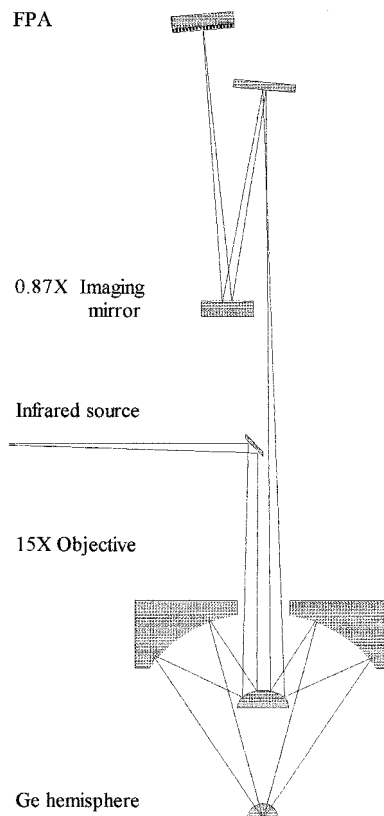


FIG. 1. Optical diagram of the microscope.

adjusted on the imaging microscope with the use of the Z-stage micrometer.

All spectra comprising the images in this investigation were collected at 16 cm^{-1} resolution and are based on a single scan. The interferometer was scanned by using a step rate of 2.5 Hz , and 40 frames were collected at each mirror position. The frame rate was 112 Hz with an integration time of 0.279 ms . The spectra and the resulting images were transformed from interferograms with the use of the existing software package on the StingRay system.

RESULTS AND DISCUSSION

One of the first parameters to be investigated was the magnification factor associated with the refractive index of the hemispherical IRE. In order to determine the magnification factor of the system with the ATR unit in place, a Nylon fiber was mounted into the ATR cartridge and its actual diameter measured with an optical microscope. This measurement was conducted through the transparent backer plate of the ATR cartridge, which allows for sample alignment. An image of the fiber was then obtained by using the infrared microscope, and this image is presented in Fig. 2A. The image is based on the amide I absorption at 1650 cm^{-1} and shows the entire 64×64 field of the array. The distance across the Nylon fiber in the infrared image is 19 pixels and that in the visible image was $22\text{ }\mu\text{m}$, demonstrating that each pixel on the detector corresponds to approximately $1.2\text{ }\mu\text{m}$ on the sample. The StingRay system employed in the current investigation possessed a magnification of $13\times$, going from the sample plane to the detector. As such, a $61\text{ }\mu\text{m}$ pixel on the de-

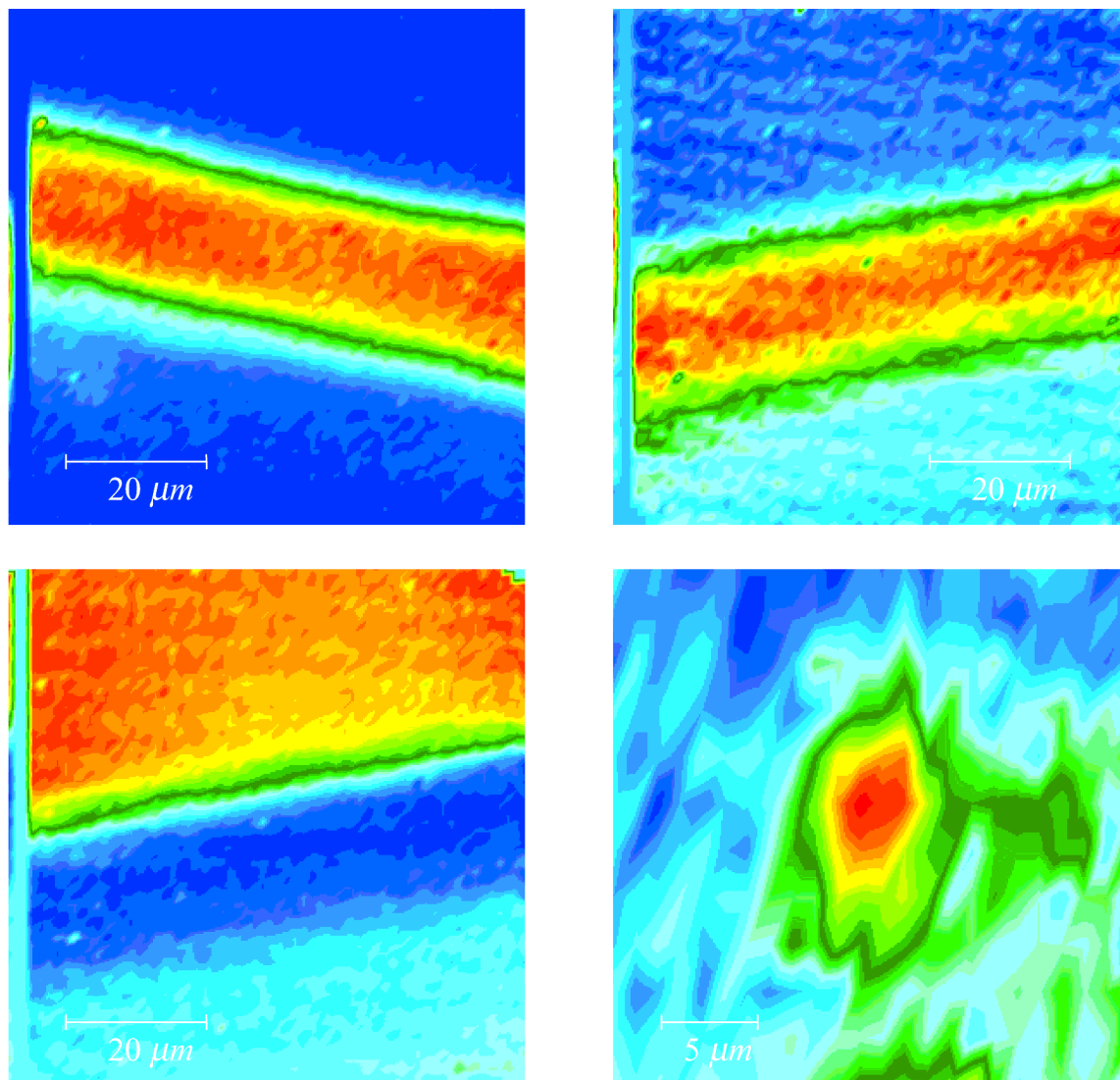


FIG. 2. (A, top left) Infrared image of a 22 μm diameter nylon fiber based on the amide I absorption at 1650 cm^{-1} . (B, top right) Infrared images of a cross-sectioned photographic film based on the amide I absorption of gelatin at 1650 cm^{-1} . (C, bottom left) Infrared image of a cross-sectioned photographic film based on the carbonyl absorption of polyvinyl acetate at 1740 cm^{-1} . (D, bottom right) Infrared image of a single red blood cell.

tector is imaged to a $4.7\text{ }\mu\text{m}$ spatial element at the sample plane. With the ATR unit in place and a magnification factor of 4 for the Ge hemisphere, one would expect each pixel on the detector to correspond to a $1.2\text{ }\mu\text{m}$ spatial element at the sample plane. The results show that the theoretical and measured values compare favorably and that the magnification factor is easily realized.

Although the previous results showed that each pixel on the detector corresponds to $1.2\text{ }\mu\text{m}$ spatial element in the sample plane, this value should not be taken as the spatial resolution of the system. The expected value for the spatial resolution d of the instrument can be obtained by using the following equation:

$$d = \frac{1.22\lambda}{n_1 \sin \theta} \quad (1)$$

The objective employed in the investigation has a numerical aperture in air of $\text{NA} = 0.6$. However, this aperture is reduced by a factor of 2 since only half of the optic is being employed to introduce the beam into the

IRE.⁵ On the basis of this value (0.3), a wavelength of $6.25\text{ }\mu\text{m}$ (1650 cm^{-1}), and a refractive index of 4.0, the theoretical spatial resolution should be $6.25\text{ }\mu\text{m}$ or approximately the wavelength of light.

The spatial resolution of the system was measured by using a cross-sectioned photographic film similar to that used by Lewis and Sommer.⁵ This film was positioned in the ATR cartridge in such a way that the interface between the polyvinyl acetate and gelatin layers was centered on the face of the IRE. The interface between these two layers was employed to generate a step function from which the spatial resolution could be determined. Infrared images presented in Figs. 2b and 2c are based on the amide I absorption at 1650 cm^{-1} and carbonyl absorption at 1740 cm^{-1} , respectively. Individual spectra (Fig. 3) were extracted from these images, and step functions were constructed with the use of the peak height for each absorption (Fig. 4). The spatial resolution was then obtained by a method similar to that of Gardiner et al.,⁷ i.e., the ordinate distance that corresponds to 5% and 95% of

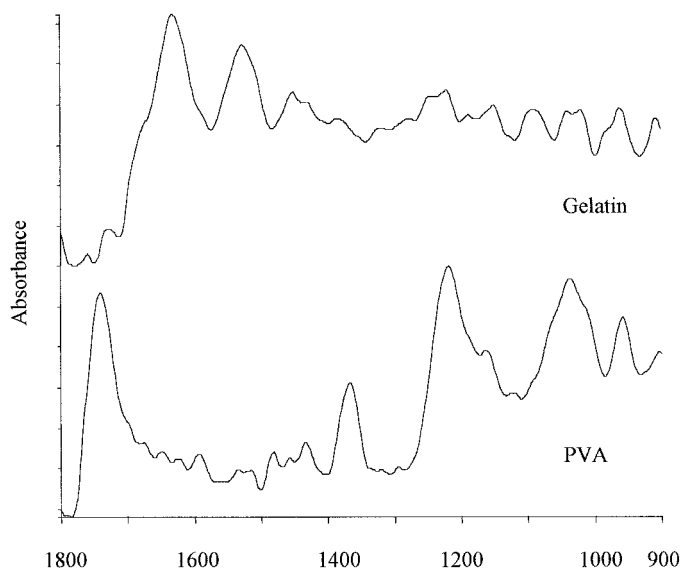


FIG. 3. Single pixel spectra extracted from the image of a cross-sectioned photographic film.

the peak height. In each case, the spatial resolution was determined to be $8\ \mu\text{m}$, which is a significant improvement over previous studies where the sampled area was significantly greater than that set by the aperture or that determined theoretically.^{5,8} Sommer and Katon previously reported on the spatial resolution of an infrared microscope in transmission mode using apertures to spatially isolate the sample.⁸ They demonstrated that, for samples in the $8\ \mu\text{m}$ size range, the actual area sampled was on the order of $48\ \mu\text{m}$, leading to a degradation factor of 6.0 (Table I). The apertures employed to isolate the small dimension yielded significant diffraction, which was the largest contributor to the degradation. Lewis and Sommer reported on an ATR approach using a conventional infrared microscope and the ATR cartridge used in this investigation.⁵ In that investigation, the ATR element and its associated magnification factor allowed one to work with aperture sizes that were four times larger, thereby reducing the deleterious effects of diffraction and subsequently lowering the degradation factor to 3.6. In the present study, no apertures are employed other than the physical size of the pixels on the array and the magnification from the sample to the detector. With this approach, it can be seen that near diffraction-limited performance can be achieved. Nakano and Kawata demonstrated slightly better spatial resolution,³ but on a system on which the measurements were relatively more difficult to implement.

CONCLUSION

The results presented in this investigation demonstrate the advantages of ATR mapping using a germanium hemisphere and a microscope outfitted with a focal plane array detector. This combination permits high signal-to-noise ratio spectra and high-contrast images to be obtained with a spatial resolution very near the diffraction limit of the microscope. The results are promising in light of the fact that spectra and images reported herein are based on a single scan. Additionally, the current geom-

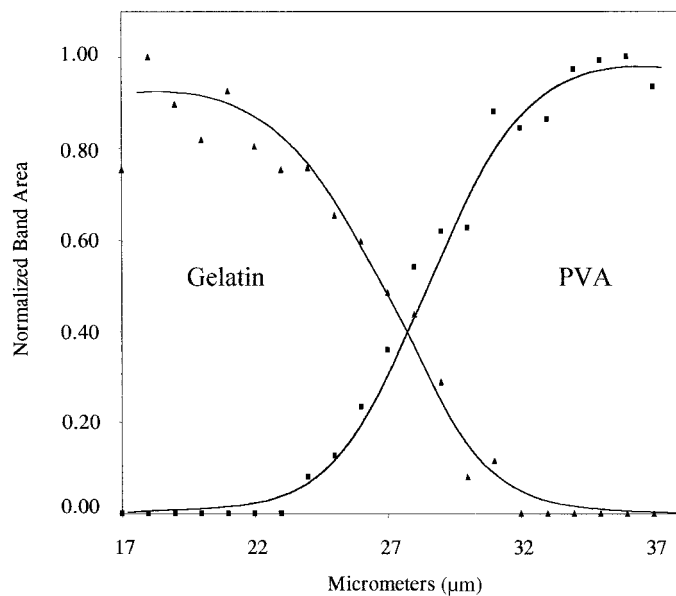


FIG. 4. Edge functions generated from the image of the cross-sectioned photographic film.

etry allows the method to be employed without instrument modification. In contrast to transmission measurements that require thin sample sections to be prepared, the ATR method permits one to work with relatively thick sample sections, thus reducing sample preparation and, hence, the expertise needed to prepare such sections. It is anticipated that the method will be a more practical alternative to current methods used to study polymer laminates and biological tissue sections, as well as bacterial colonies with tens of individual bacteria present. For example, Lang et al. have reported on the use of ATR microspectroscopy and principal component regression analysis to distinguish between Gram-positive and -negative bacteria.⁹

To put things in perspective, the signal that one detector element is sensing arises from a sample volume element, which is $\sim 11\ \text{fL}$. This volume element is based on a spatial resolution of $8\ \mu\text{m}$, a penetration depth of $1\ \mu\text{m}$, and a conical geometry for the evanescent beam present at the sample/IRE interface. Assuming a density of $1.2\ \text{grams/cm}^3$, this volume element translates into a mass of $13\ \text{fg}$. Figure 2D exhibits the image of a single red blood cell and is based on the amide I absorption. The image was collected by placing a drop of blood on the crystal and once again collecting a single scan. Single red blood cells were previously studied by Dong et al. with the use of a conventional transmission microscope.¹⁰ The image provides not only molecular information but also mor-

TABLE I. Summary of spatial resolution for various modes of measurement.

Method	Sample size (μm)	Spatial resolution (μm)	Degradation factor
Normal transmission ^a	8.0	48	6.0
Point ATR ^b	6.0	22	3.6
Imaging ATR	6.0	8.0	1.3

^a For experimental details and conditions refer to Ref. 8.

^b For experimental details and conditions refer to Ref. 5.

phological information in that the size of the cell based on pixel occupancy is approximately 8 μm , a size corresponding precisely to that of a normal human erythrocyte.

Finally, two instrumental factors can be employed to enhance the performance of the system and extend its capabilities into subwavelength spatial resolution. First, the beamsplitter employed in the microscope is the aperture splitting type. This geometry uses only half of the microscope objective's total aperture with a concomitant reduction in spatial resolution. By using a conventional beamsplitter (germanium-coated KBr) and filling the aperture, one can increase the spatial resolution by a factor of 2 over the present conditions. Although the signal would be reduced by this approach, signal averaging could be employed to regain image contrast.

ACKNOWLEDGMENTS

The authors gratefully acknowledge the support of Ford Motor Company, 3M, Kodak, and Procter and Gamble.

1. N. J. Harrick, M. Milosevic, and S. L. Berets, *Appl. Spectrosc.* **45**, 944 (1991).
2. J. Coates and J. Reffner, *Spectroscopy* **15**, 19 (2000).
3. T. Nakano and S. Kawata, *Scanning* **16**, 368 (1994).
4. L. Lewis and A. J. Sommer, *Appl. Spectrosc.* **53**, 375 (1999).
5. L. Lewis and A. J. Sommer, *Appl. Spectrosc.* **54**, 324 (1999).
6. K. P. J. Williams, G. D. Pitt, D. N. Batchelder, and B. J. Kip, *Appl. Spectrosc.* **48**, 232 (1994).
7. D. J. Gardiner, M. Bowden, and P. R. Graves, *Philos. Trans. R. Soc. London, Ser. A* **320**, 295 (1986).
8. A. J. Sommer and J. E. Katon, *Appl. Spectrosc.* **45**, 527 (1991).
9. P. L. Lang, J. L. Hodges and C. D. Keffer, *Cell. Molec. Biol.*, paper to be published.
10. A. Dong, R. G. Messerschmidt, J. A. Reffner, and W. S. Coughney, *Biochem. Biophys. Res. Commun.* **156**, 752 (1988).